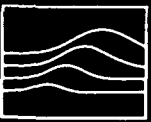


✓ 2



Mission Research Corporation

MRC/WDC-R-196

AD-A222 048

THE THEORY AND SIMULATION OF PLASMOID FORMATION AND PROPAGATION

Approved for public release;
distribution unlimited.

John Brandenburg
Gary Warren
Richard Worl

February 1989

AIR FORCE OFFICE OF SCIENTIFIC RESEARCH (AFOSR)
NATIONAL TECHNICAL INFORMATION SERVICE (NTIS)
3501 MARKET STREET, PHOTODUPLICATION SERVICE
SPRINGFIELD, VIRGINIA 22161-4302
This document is available to the public and is
not subject to copyright law AFR 190-12.
FOR INFORMATION CONTACT:
CIVIL TECHNICAL INFORMATION DIVISION

Prepared for: Physical and Geophysical Sciences Directorate
AFOSR/NP, Building 410
Bolling AFB, D.C.
Attention: Major Bruce L. Smith

Contract No. F49620-88-C-0049

Prepared by: MISSION RESEARCH CORPORATION
8560 Cinderbed Road, Suite 700
Newington, VA 22122
(703) 339-6500

DTIC
ELECTE
MAY 30 1990
S B D
Cg

Research sponsored by the Air Force Office of Scientific Research (AFOSR), under Contract F49620-88-C-0049. The United States Government is authorized to reproduce and distribute reprints for governmental purposes notwithstanding any copyright notation hereon.

UNCLASSIFIED

SECURITY CLASSIFICATION OF THIS PAGE

REPORT DOCUMENTATION PAGE

Form Approved
OMB No. 0704-0188
Exp. Date: Jun 30, 1986

1a. REPORT SECURITY CLASSIFICATION UNCLASSIFIED			1b. RESTRICTIVE MARKINGS			
2a. SECURITY CLASSIFICATION AUTHORITY N/A Since Unclassified			3. DISTRIBUTION/AVAILABILITY OF REPORT Approved for public release; distribution unlimited.			
2b. DECLASSIFICATION/DOWNGRADING SCHEDULE N/A Since Unclassified						
4. PERFORMING ORGANIZATION REPORT NUMBER(S) MRC/WDC-R-196			5. MONITORING ORGANIZATION REPORT NUMBER(S) AFOSR-TR-90-0535			
6a. NAME OF PERFORMING ORGANIZATION Mission Research Corporation		6b. OFFICE SYMBOL (if applicable)		7a. NAME OF MONITORING ORGANIZATION <i>Same as 8a</i>		
6c. ADDRESS (City, State, and ZIP code) 8560 Cinderbed Road, Suite 700 Newington, VA 22122			7b. ADDRESS (City, State, and ZIP code) <i>Same as 8c</i>			
8a. NAME OF FUNDING/SPONSORING ORGANIZATION AFOSR Physical & Geophysical Sci. Dir.		8b. OFFICE SYMBOL (if applicable) <i>NIP</i>		9. PROCUREMENT INSTRUMENT IDENTIFICATION NO. <i>F49620-88-C-0049</i>		
8c. ADDRESS (City, State, and ZIP code) AFOSR/NP, Building 410 Bolling AFB, D.C. 20332-6448			10. SOURCE OF FUNDING NUMBERS			
			PROGRAM ELEMENT NO. <i>61102A</i>	PROJECT NO. <i>2301</i>	TASK NO. <i>A78</i>	WORK UNIT ACCESSION NO.
11. TITLE (Include Security Classification) PROGRESS ON THE THEORY & SIMULATION OF PLASMOID FORMATION & PROPAGATION (21)						
12. PERSONAL AUTHOR(S) John E. Brandenburg, Gary Warren, Richard Worl						
13a. TYPE OF REPORT Final Technical Report		13b. TIME COVERED From <i>1 JAN 88-30 Sep 89</i>		14. Date of Report (Year, Month, Day) January 1990		15. PAGE COUNT 33
16. SUPPLEMENTARY NOTATION Attn: Dr. Robert Barker						
17. COSATI CODES			18. SUBJECT TERMS (continue on reverse if necessary and identify by block number) Plasmoid, Arrow plasmoid, Virial theorem, EM PIC Code, Analytic approximation, MAGIC, SOS			
FIELD	GROUP	SUB-GROUP				
			19. ABSTRACT (Continue on reverse if necessary and identify by block number) A summary of progress on the theory and simulation of plasmoid formation and propagation at Mission Research Corporation is presented. Progress occurred in two areas. First, an analytical model of core-halo dynamics was derived for an arrow-type plasmoid. This model predicts halo expansion that is approximately linear in time with a velocity proportional to the core ion sound speed and a core expansion that is logarithmic in time. Second, simulation efforts have successfully formed and propagated plasmoids with core and halo structure.			
20. DISTRIBUTION AVAILABILITY OF ABSTRACT <input checked="" type="checkbox"/> Unclassified/Unlimited <input checked="" type="checkbox"/> Same as RPT. <input checked="" type="checkbox"/> DTIC Users			21. ABSTRACT SECURITY CLASSIFICATION UNCLASSIFIED			
22a. NAME OF RESPONSIBLE INDIVIDUAL <i>Dr Robert J. Barker</i>			22b. TELEPHONE (Include Area Code) <i>202/767-5011</i>		22c. OFFICE SYMBOL <i>NIP</i>	

Copy 11

MRC/WDC-R-196

THE THEORY AND SIMULATION OF PLASMOID FORMATION AND PROPAGATION

John Brandenburg
Gary Warren
Richard Worl

February 1989

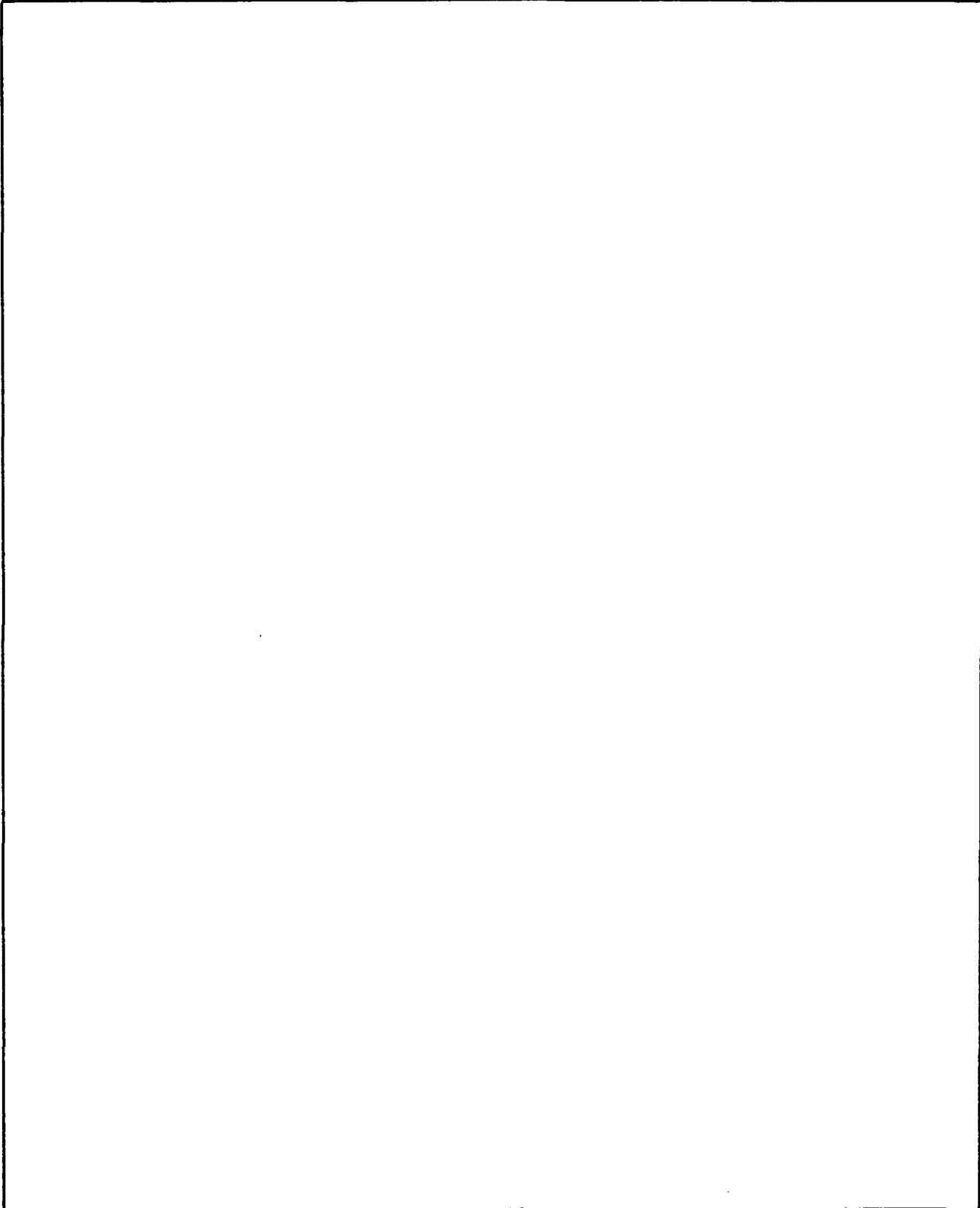
Prepared for: Physical and Geophysical Sciences Directorate
AFOSR/NP, Building 410
Bolling AFB, D.C.
Attention: Major Bruce L. Smith

Contract No. F49620-88-C-0049

Prepared by: MISSION RESEARCH CORPORATION
8560 Cinderbed Road, Suite 700
Newington, VA 22122
(703) 339-6500

UNCLASSIFIED

SECURITY CLASSIFICATION OF THIS PAGE



SECURITY CLASSIFICATION THIS PAGE

UNCLASSIFIED

TABLE OF CONTENTS

Section	Page
LIST OF ILLUSTRATIONS	iv
1 INTRODUCTION	1-1
2 A MODEL OF CORE-HALO DYNAMICS IN A PROPAGATING PLASMOID	2-1
2.1 BASIC EQUATIONS	2-1
2.2 APPROXIMATE SOLUTION OF THE SYSTEM	2-3
2.3 PROPERTIES OF THE APPROXIMATE SOLUTION	2-5
3 SIMULATIONS OF PLASMOID FORMATION AND PROPAGATION	3-1
3.1 PROGRESS IN SIMULATIONS OF PLASMOIDS	3-1
3.2 A TECHNIQUE FOR SUCCESSFUL FORMATION OF PLASMOIDS	3-1
4 THREE-DIMENSIONAL PLASMOID SIMULATIONS	4-1
4.1 SIMULATIONS USING THE CODE SOS	4-1
4.2 RESULTS OF SIMULATIONS	4-2
5 SUMMARY AND CONCLUSIONS	5-1



or	
DTIC TAB	<input checked="" type="checkbox"/>
Unannounced	<input type="checkbox"/>
Justification	<input type="checkbox"/>
By _____	
Distribution/	
Availability Codes	
Dist	Avail and/or Special
A-1	

LIST OF ILLUSTRATIONS

Figure	Page
1.1 An arrow plasmoid. This plasmoid model was first proposed by Tom Lockner of Sandia National Laboratories	1-2
2.1 A curve of halo radius versus time from the analytic solution for an $I_0 = 22\text{kA}$ plasmoid	2-6
2.2 A curve of core radius versus time from the analytic solution for an $I_0 = 22\text{kA}$ plasmoid	2-7
2.3 Curves of core radius (labeled inner radius) and halo radius (labeled outer radius) from numerical solution of an $I_0 = 22\text{kA}$ plasmoid at Sandia National Laboratories. Figures are taken from Reference 2	2-8
3.1 Steps in the sequence for forming an arrow plasmoid, (A) end cap formation, no net currents, (B) annular halo and core formation net currents included by relative velocities between ions and electrons. (C) second end cap formation. Solid arrows indicate net currents, open arrows indicate center of mass motion	3-3
3.2 Ion position plots in a plasmoid after several meters of propagation. Note possible halo formation in plasmoid	3-5
3.3 Radial integrals of current and charge in a simulated plasmoid; note that both integrals peak at roughly .15 meters radius and then decline to near zero. This shows core-halo division as expected. Note also that, inexplicably, net current is negative, while net charge is positive	3-6
4.1 The $x_2, x_3 (z,y)$ gridding of the plasmoid problem. Gridding in the $x_1 (x)$ direction is uniform. Only the top half of the x_2, x_3 gridding is shown	4-3
4.2 The initial beams for forming the plasmoid as they are emitted	4-4

LIST OF ILLUSTRATIONS (Concluded)

Figure		Page
4.3	Final trajectory plots for a plasmoid. The plasmoid is seen impacting on the wall at 2.5 meters. The trail of particles behind the plasmoid is a group of electrons and ions emitted after main beam shut down and are considered spurious since their total charge and current is negligible	4-5
4.4	Cross section of the plasmoid at impact at 2.5 meters. The cross section shows clear core-halo structure with the suggestion of $m = 4$ filamentation in the halo	4-6

SECTION 1

INTRODUCTION

During the years 1988-1989, progress on understanding plasmoid formation and propagation occurred in two areas of inquiry: an analytical model for the dynamics of the core and halo of a long, thin plasmoid and simulation models of plasmoid formation and propagation.

An analytic approximation was found for the internal dynamics of a long, thin propagating plasmoid. The plasmoid model studied has been termed the "Arrow" model¹ and consists of a confined, current carrying core and an expanding halo carrying return currents (Figure 1.1). The analytic model has the basic result that the halo expansion velocity is nearly constant and determined by the sound speed in the core,

$$V_o = V_{th} \left(2 \ln \frac{R_o}{a_o} \right)^{1/2}, \quad (1.1)$$

where $V_{th} = \left(\frac{kT_e}{M_{ion}} \right)^{1/2}$ is the sound speed, kT_e is the electron temperature, M_{ion} is the ion mass and R_o and a_o are the initial halo and initial core radii respectively. From this model the core has been found to expand slowly with respect to the halo,

$$a = a_o \left(\frac{\ln R/a_o}{\ln(R_o/a_o)} \right)^{3/2}, \quad (1.2)$$

where a is the core radius and R is the halo radius. So this gives

$$a \propto (\ln t)^{3/2} \quad (1.3)$$

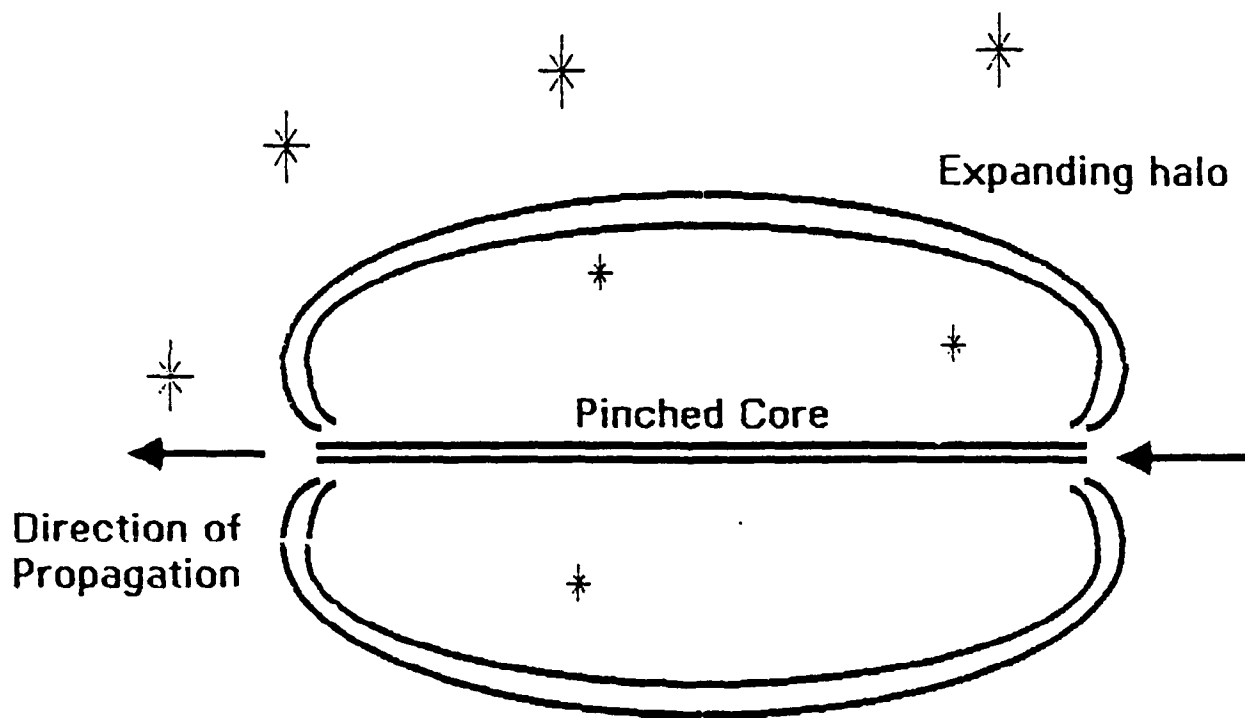


Figure 1.1. An arrow plasmoid. This plasmoid model was first proposed by Tom Lockner of Sandia National Laboratories.

for $R \gg a$. This model demonstrates that the expansion rate of the plasmoid halo is a controllable parameter in the long, thin limit and that, within this limit, the core radius will not change much in time.

Simulations of the formation and propagation of an arrow type plasmoid have been performed in two-and-one-half dimensions using the EM PIC code MAGIC, and in three dimensions with the EM PIC code SOS. After many attempts to launch a plasmoid, a prescription was found for forming a plasmoid that would propagate and form a halo-core configuration. This effort resulted in a short movie which now exists in the form of a videotape.

In the remainder of this report, detailed discussions of the analytic model will be given as well as a discussion of progress in simulation efforts. The final chapter will summarize the results.

SECTION 2

A MODEL OF CORE-HALO DYNAMICS IN A PROPAGATING PLASMOID

As part of the research progress made in 1988 and 1989, a useful analytic approximation to the dynamics of the core and halo of an arrow-type plasmoid (see Figure 1.1) has been developed. This model agrees well with numerical simulations and allows rapid estimation of the expansion of such a system during free-space propagation.

The model demonstrates that the speed of expansion of a halo is nearly constant and is well approximated by

$$V_o = V_{th} (2 \ln (R_o/a_o))^{1/2} , \quad (2.1)$$

where V_{th} is the thermal velocity of the ions and R_o and a_o are the initial halo and core radii, respectively. Based on this model, it appears that plasmoids can be made to propagate long distances with a tightly pinched core if plasma temperatures are kept low.

2.1 BASIC EQUATIONS

We begin by assuming an arrow-type plasmoid as shown in Figure 1.1 with a core satisfying an equilibrium relation,

$$I^2/c^2 = 2NkT , \quad (2.2)$$

where I is the plasmoid current, c is the speed of light, kT is the gas temperature (assuming identical temperatures for both ions and electrons), and N is the total number of particles per unit length in the core.

Such a core equilibrium is not possible without a path for the return current. In the arrow plasmoid, this return current path is provided by the halo. However, the halo encloses the magnetic field of the core and will expand due to magnetic pressure.

The radius of the halo (assuming it is an infinitesimal layer) is found for the $\mathbf{J} \times \mathbf{B}$ force on a single ion to be

$$M_{\text{ion}} \partial_t^2 R = e \vec{V}_d \times \vec{B}_\theta, \quad (2.3)$$

where R is the halo radius, M_{ion} is the ion mass, eV_d is the current divided by the number of charge carriers per unit length, e is the electron charge, and B_θ is the magnetic field, $B_\theta = 2I/cR$. We have

$$\partial_t^2 R = \frac{2I^2}{Nmc^2 R}. \quad (2.4)$$

The magnetic flux in the halo-core system is assumed to be conserved and the plasmoid is assumed to be long and thin. This leads to the expression,

$$I = I_0 \ln(R/a_0) / \ln(R_0/a_0), \quad (2.5)$$

where a is the core radius.

The sound transit times in the core are assumed to be very short so that the core can adjust continuously to the change in current. This will mean that Equation 2.2 will be in effect continuously. The core pressure is given by the adiabatic law,

$$P = P_o \left(\frac{n}{n_o} \right)^{5/3}, \quad (2.6)$$

where n is the number density, or number of charge carriers per unit length in the core divided by the area of the core, $n = N/\pi a^2$. Using $P = nkT$, we have

$$kT = kT_o \left(\frac{n}{n_o} \right)^{2/3}. \quad (2.7)$$

Using Equation 2.2, we have

$$\frac{I}{I_o} = (a_o/a)^{2/3}, \quad (2.8)$$

which gives us, through Equation 2.5,

$$a = a_o (\ln(R/a) / \ln(R_o/a_o))^{3/2}. \quad (2.9)$$

2.2 APPROXIMATE SOLUTION OF THE SYSTEM

We can now write the equations for the halo-core dynamics,

$$\partial_t^2 R = \frac{2I_o^2}{Nmc^2} \left[\frac{(\ln(R_o/a_o))}{\ln(R/a)} \right]^2 \frac{1}{R}, \quad (2.10)$$

$$a = a_o (\ln(R/a) / \ln(R_o/a_o))^{3/2}. \quad (2.11)$$

In Equation 2.11, we can see that a changes very little as R changes. Therefore, we can obtain an approximate solution by letting a be constant in Equation 10. We obtain

$$\partial_t^2 R = \frac{C}{(\ln R/a_0)^2} \frac{1}{R} \quad (2.12)$$

with $C = (2 \ln R_0/a_0)^2 I_0^2 / Nmc^2$. This can be integrated once by multiplying both sides by $\partial_t R$. We then obtain

$$\frac{1}{2} (\partial_t R)^2 = C / \ln(R/a_0) \Big|_{R_0}^R . \quad (2.13)$$

This can be written

$$\partial_t R = V_0 \left(1 - \frac{\ln(R_0/a_0)}{\ln(R/a_0)} \right)^{1/2} , \quad (2.14)$$

where we have,

$$V_0 = (4I_0^2 \ln(R_0/a_0) / Nmc^2)^{1/2} . \quad (2.15)$$

By Equation 2.2, this can be written

$$V_0 = (2 \ln(R_0/a_0) kT/m)^{1/2} . \quad (2.16)$$

In the limit $R \gg R_0$, we can expand binomially to first order,

$$\partial_t R = V_0 \left(1 - 1/2 \frac{\ln(R_0/a_0)}{\ln(R/a_0)} \right) . \quad (2.17)$$

In this limit, the logarithmic term will change very slowly; therefore, we can substitute $R = V_0 t^*$ where $t^* = t + t_0$ and $t_0 = R_0/V_0$. We integrate to obtain

$$R = V_0 t^* - \frac{1}{2} a_0 \ln(R_0/a_0) (L_i(\tau) - L_i(R_0/a_0)) \quad (2.18)$$

where $\tau = V_o t^* / a_o$, and $L_i(\tau)$ is the logarithmic integral function. This is our approximate solution in the limit $R \gg R_o$.

2.3 PROPERTIES OF THE APPROXIMATE SOLUTION

The approximations used to find Equation 2.18 are certainly good in the limit $R \gg R_o$; however, they must give an over-estimate of R . The quantity a will always be larger than a_o , making the quantity R/a smaller and the quantity $\ln(R_o/a_o) / \ln(R/a)$ larger. Also, the binomial expansion of the square root will over-estimate the value of small R . Thus, the approximate integral of Equation 2.14 will be an over-estimate of the true integral. The most important feature of our analytic solution is that it predicts $R \cong V_o t$; that is that R will expand at nearly a constant velocity, and that this velocity is just a geometric factor, $(\ln R_o/a_o)^{1/2}$, times the core ion thermal velocity. This shows that cooling the core plasma and lowering the aspect ratio of the halo and core radii can strongly reduce the expansion of the halo, allowing long-distance propagation.

The accuracy of the analytic solution can be seen by comparing it with numerical solutions for a plasmoid system found at Sandia Laboratories and described in Reference (2). For the case, $I_o = 22\text{kA}$, $R_o = 1\text{ m}$, $a_o = .1\text{ m}$, we obtain the result, $kT = 100\text{eV}$. Best agreement between the Sandia results and the analytic solution was obtained by reducing I_o in the analytic solution by a factor of .825. This can be understood as compensation for early core expansion, which will lower current. When this factor is applied, it can be seen in Figures 2.1 - 2.3 that agreement between the Sandia results and the analytic model is excellent.

The core expansion rate is slow and is given approximately from Equations 2.9 and 2.18 as

$$a^2 \cong a_o (\ln((V_o t^*)/a) / \ln(R_o/a_o))^{3/2} \quad (2.19)$$

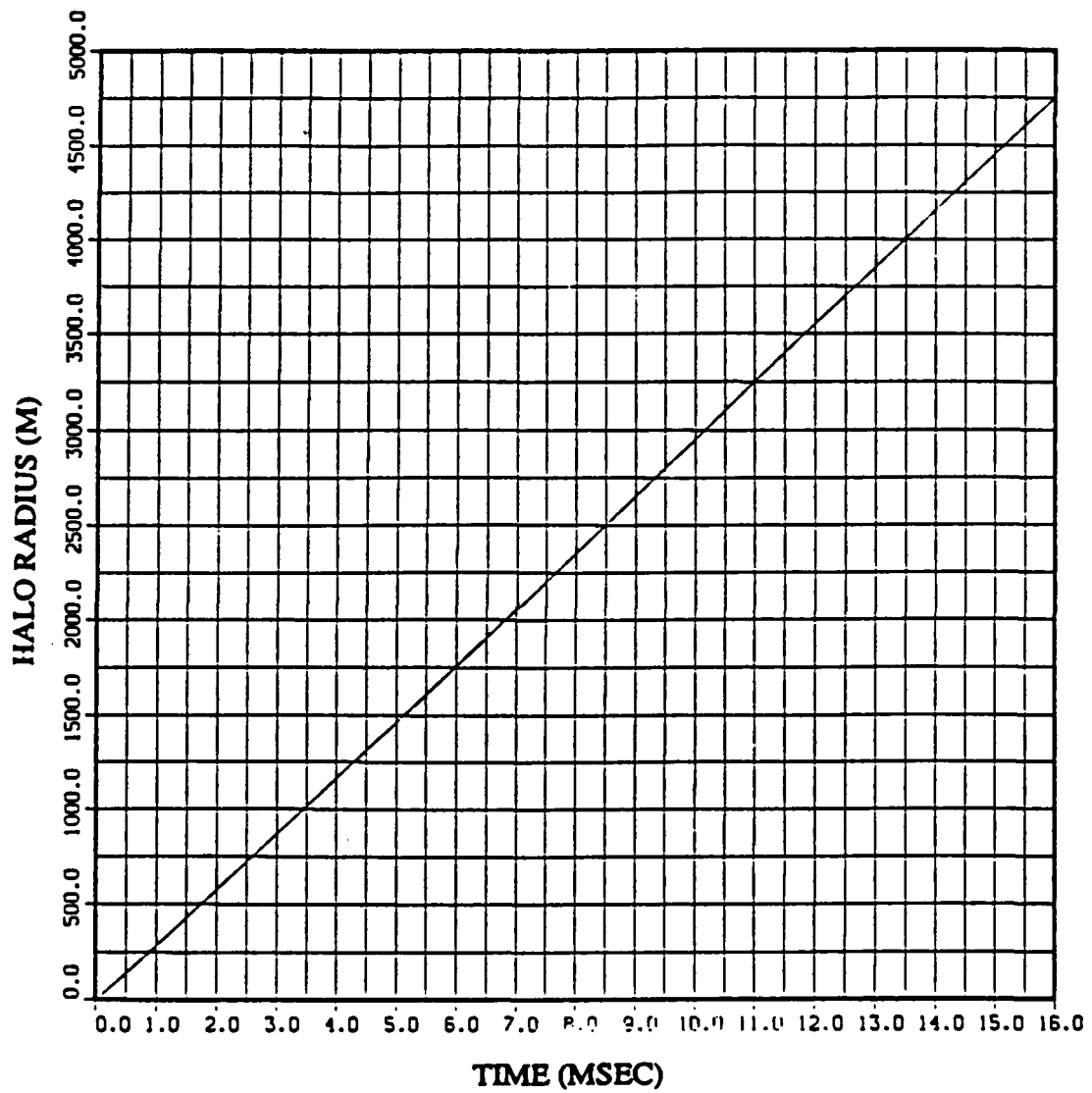


Figure 2.1. A curve of halo radius versus time from the analytic solution for an $I_0 = 22\text{kA}$ plasmoid.

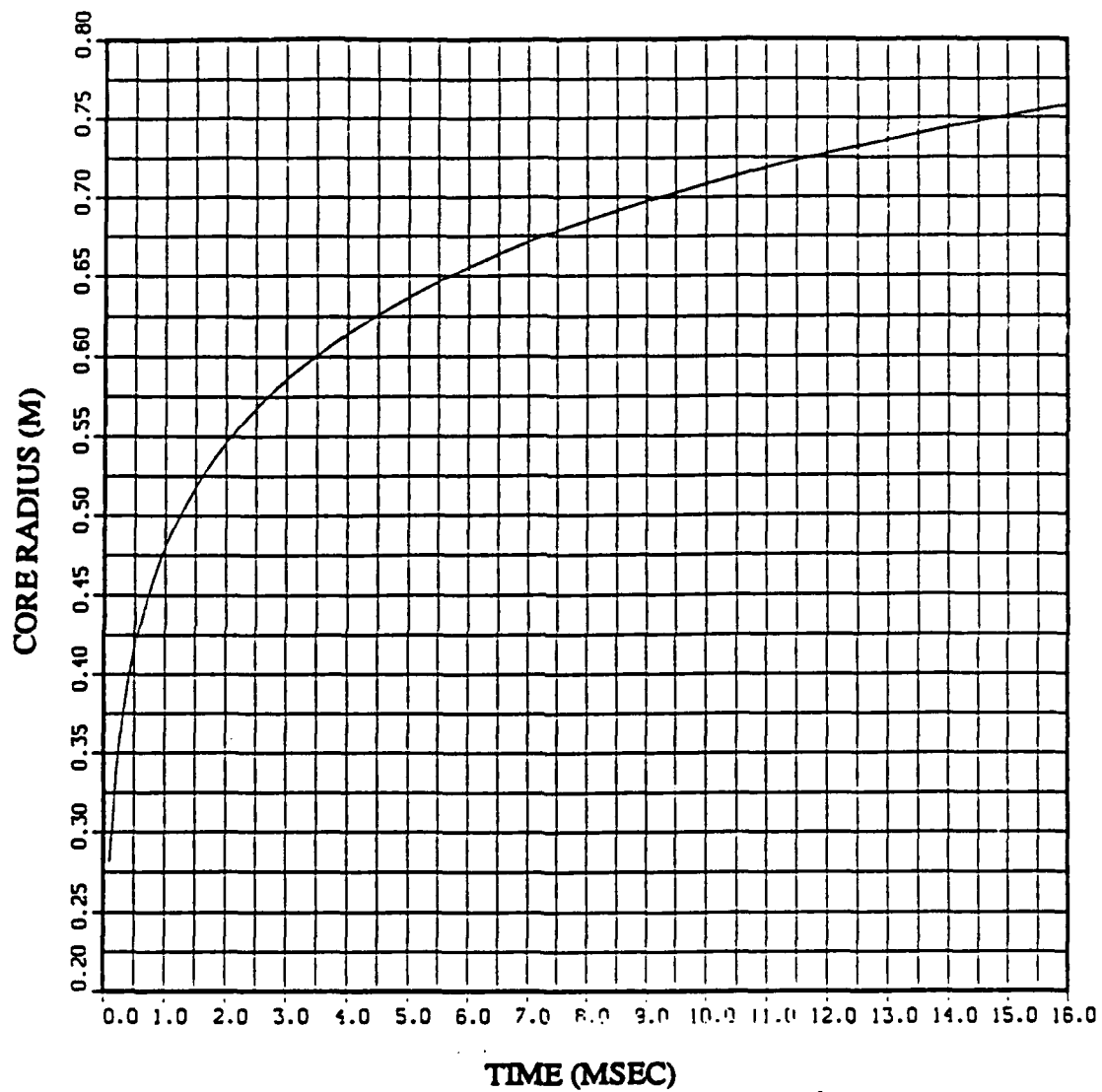


Figure 2.2. A curve of core radius versus time from the analytic solution for an $I_0 = 22\text{kA}$ plasmoid.

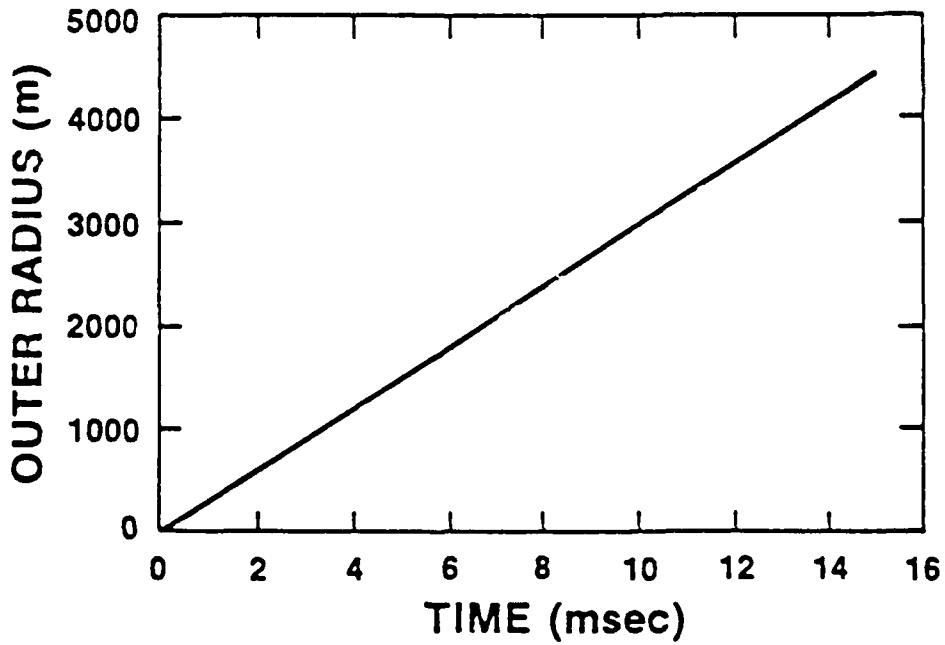
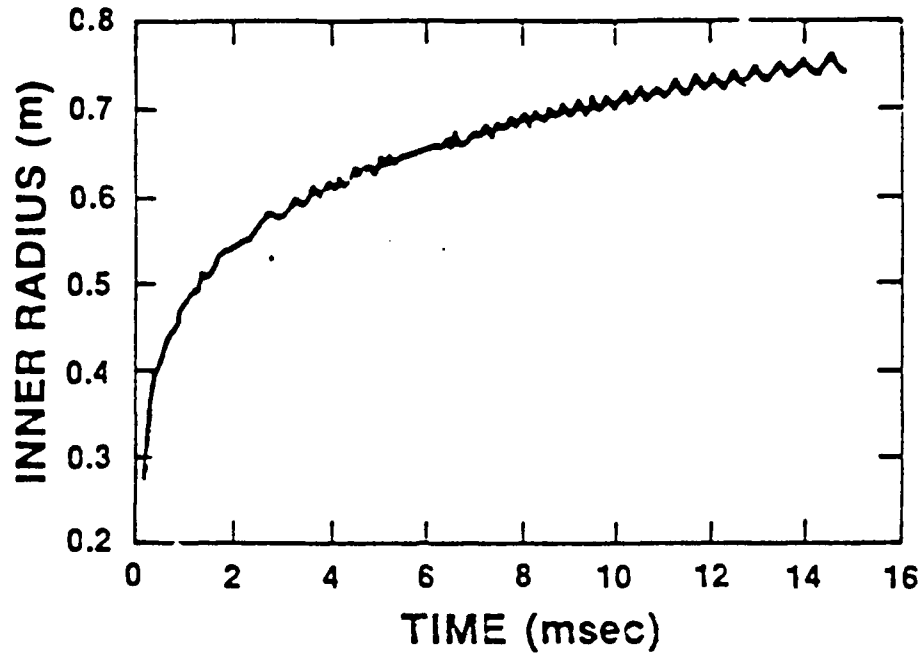


Figure 2.3. Curves of core radius (labeled inner radius) and halo radius (labeled outer radius) from numerical solution of an $I_0 = 22\text{kA}$ plasmoid at Sandia National Laboratories. Figures are taken from Reference 2.

$$\partial_t a \cong 3/2 \frac{a_0}{t^*} \left(\frac{a}{a_0} \right)^{1/2} . \quad (2.20)$$

SECTION 3

SIMULATIONS OF PLASMOID FORMATION AND PROPAGATION

3.1 PROGRESS IN SIMULATIONS OF PLASMOIDS

Efforts to simulate plasmoids were begun on the Mission Research Corporation MicroVax using the fully electromagnetic particle-in-cell code MAGIC.³ The code MAGIC was modified to emit beams of particles corresponding to models of plasmoid structure worked out in previous research.² The MicroVax was used because it allowed rapid turnaround of calculations and many short-range propagation calculations to be done at a minimum cost. These calculations laid the groundwork for larger and longer calculations to be done on a Cray supercomputer. These calculations were successful and produced plasmoids that formed and propagated several meters as a unit. However, it was found that the emitted beams had to be programmed carefully to avoid complete disintegration of the plasmoid. In particular, it was found that large build-ups of space charge, however transient, had to be avoided in order to form a stable plasmoid. The process can be summarized as the creation of a pattern of flowing net currents with no breaks in the plasma carrying the current. Once this was learned, the MAGIC calculations were transferred to the Cray and this resulted in the production of a movie showing the formation and propagation of a plasmoid.

3.2 A TECHNIQUE FOR SUCCESSFUL FORMATION OF PLASMOIDS

The successful formation of plasmoids for MAGIC simulations requires a programmed emission of ion and electron beams whose properties are correlated. Central to this attempt to form plasmoids was the concept that plasmoids are a natural and fundamental mode of propagating plasmas in vacuum, and that if conditions in

a system of ions and electrons were produced that were sufficiently close to an ideal "plasmoid mode," then the system would rapidly relax into the ideal plasmoid mode and propagate. Therefore, it was expected that if the electron and ion beams were to form a plasmoid, the beams would have to have correlated velocities and densities plus some excess particles that would allow the system to dissipate energy in relaxation.

After many attempts, it was found that successful formation of a plasmoid required firing a sequence of ion and electron beams with "arrow-like" spatial and velocity profiles and a slight excess of negative charge in the halo region. To form an arrow-like plasmoid, we must launch a core and halo region containing counter-flowing and globally cancelling net currents and two "endplates" to provide an unbroken path for currents to flow. Ideally, this plasmoid will be formed as a cylinder surrounded by an annulus with plates on the ends. Upon propagation, the annulus will expand, forming the halo, and the cylinder will contract to form a pinched core. The sequence of events for forming an arrow plasmoid is shown in Figure 3.1.

Temperature is given both electrons and ions so the core will satisfy the equilibrium virial relation¹,

$$I^2/c^2 - Q^2 = 2NkT, \quad (3.1)$$

in all frames. Here, I and Q are net current and charge per unit length, respectively (typically, $Qc/I \ll 1$).

The ion and electron beams were originally emitted together with zero velocity difference for a short period over a broad radial area with a spatial density profile,

$$n = n_0(1 - r^2/r_0^2), \quad (3.2)$$

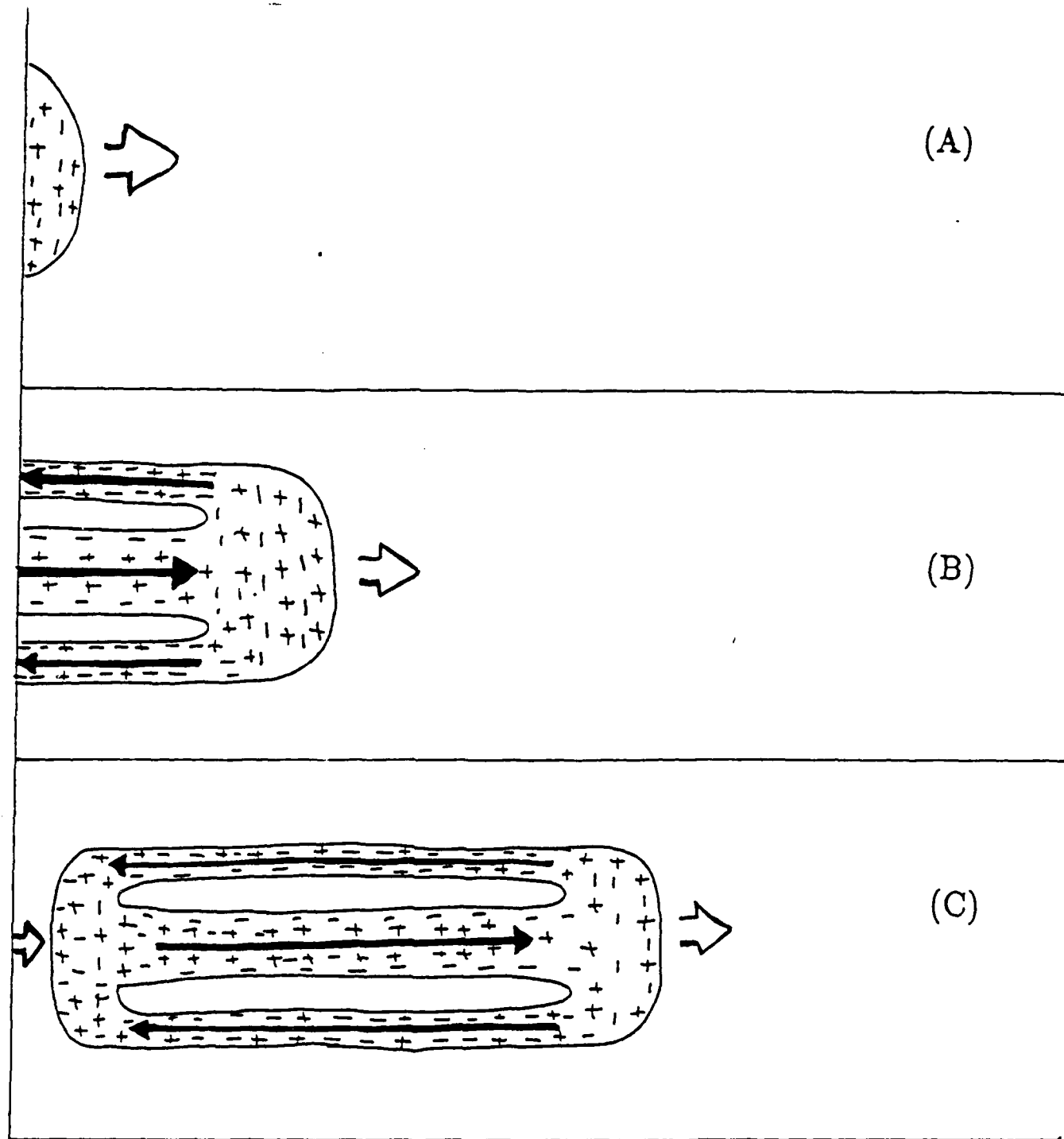


Figure 3.1. Steps in the sequence for forming an arrow plasmoid, (A) end cap formation, no net currents, (B) annular halo and core formation net currents included by relative velocities between ions and electrons. (C) second end cap formation. Solid arrows indicate net currents, open arrows indicate center of mass motion.

where n is the particle density, n_0 is a peak density, r is a radius, and r_0 is a radius where the beam density goes to zero. This quadratic profile for the beam was found to be necessary for plasmoid formation; square profile beams exploded immediately. As shown in Figure 3.1, the broad area of plasma propagating forward is the front endplate of the arrow. The beams of ions and electrons were then emitted for a period with a gap in the density pattern at $r/r_0 = \frac{1}{2}$ (the radius of 1/2 beam current for quadratic profile), and ions inside this radius were given a slight enhancement of both velocity and density over the electrons. Outside the gap radius, electrons were given a slight density enhancement (slightly more than required to balance the core ion enhancement) and a slight velocity enhancement. This pattern created a distinct core and halo region with oppositely flowing and globally cancelling currents. The final sequence of beam emission was a repeat of the front endplate beam to allow for a back endplate, thus providing an unbroken region of plasma to connect the core and halo.

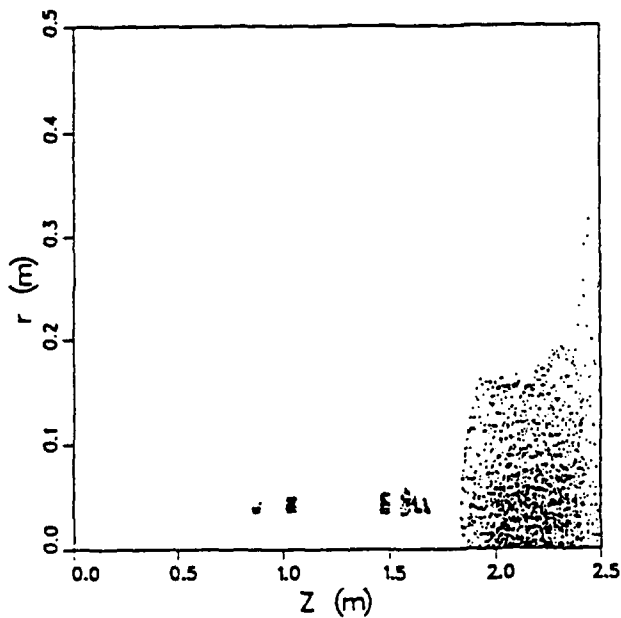
Results of these programmed formation sequences can be seen in Figures 3.2 - 3.3. These figures show the propagation, current, and charge distribution of a plasmoid. At the end of the simulation, distinct halo and core regions appear to have formed, with the core expanding slightly and the halo expanding rapidly, but maintaining an unbroken path for current. In addition, radial integrals of current and charge show that although large regions of current and charge exist in the plasmoid, its net current and charge is very small. Core expansion is expected in these simulations as shown by our model in Chapter 2. However, in longer propagation runs, it is expected that the core expansion rate will drop markedly, as is also predicted by the model.

Simulations of these plasmoids were performed on a Cray, and we produced in a short movie. This movie has been included as part of this report.

The slight imbalance of negative charge in the outer halo is to insure that the halo will be a net emitter of particles and thus energy. As was discussed previously, the plasmoid is conceived of as a relaxed state. This means it must have a way of

MAGIC VERSION: SEPTEMBER 1988 DATE: 9/28/88
SIMULATION: BENNET PLASMOID CREATION 2.22

PHASE-SPACE PLOT OF Z VS. R AT TIME: 2.03E-08 SEC
SPECIES NUMBER: 2 O/M RATIO: 9.579E+08
PZ WINDOW: -5.00E+08 TO 5.00E+08
PR WINDOW: -5.00E+08 TO 5.00E+08
PTMETHA WINDOW: -2.00E+09 TO 2.00E+09



MAGIC VERSION: SEPTEMBER 1988 DATE: 9/28/88
SIMULATION: BENNET PLASMOID CREATION 2.22

TRAJECTORY PLOT OF IONS (ISPC = 2)
FROM TIME 2.018E-08 SEC TO 2.031E-08 SEC

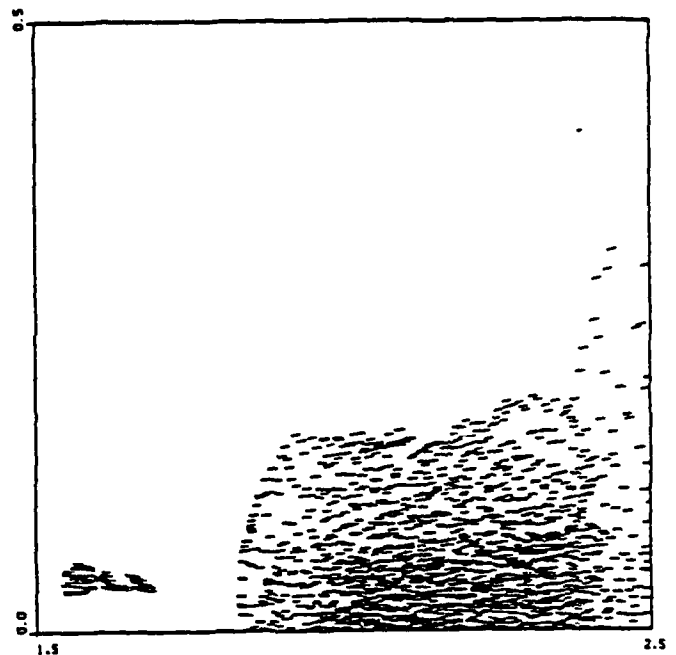
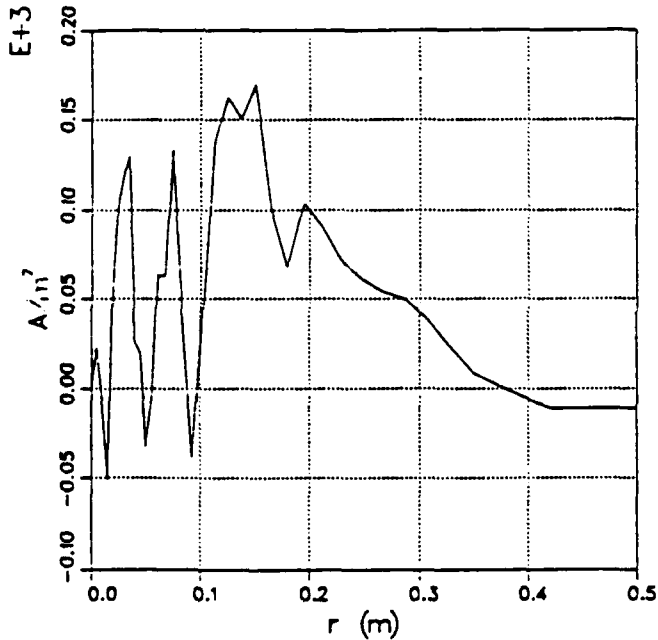


Figure 3.2. Ion position plots in a plasmoid after several meters of propagation. Note possible halo formation in plasmoid.

MAGIC VERSION: SEPTEMBER 1988 DATE: 9/28/88
SIMULATION: BENNET PLASMOID CREATION 2.22

RANGE PLOT AT TIME: 2.03E-08 SEC
RADIAL INTEGRAL OF J1 COMPONENT
RANGING FROM (225,2) TO (225,40)



MAGIC VERSION: SEPTEMBER 1988 DATE: 9/28/88
SIMULATION: BENNET PLASMOID CREATION 2.22

RANGE PLOT AT TIME: 2.03E-08 SEC
RADIAL INTEGRAL OF Q0 COMPONENT
RANGING FROM (225,2) TO (225,40)

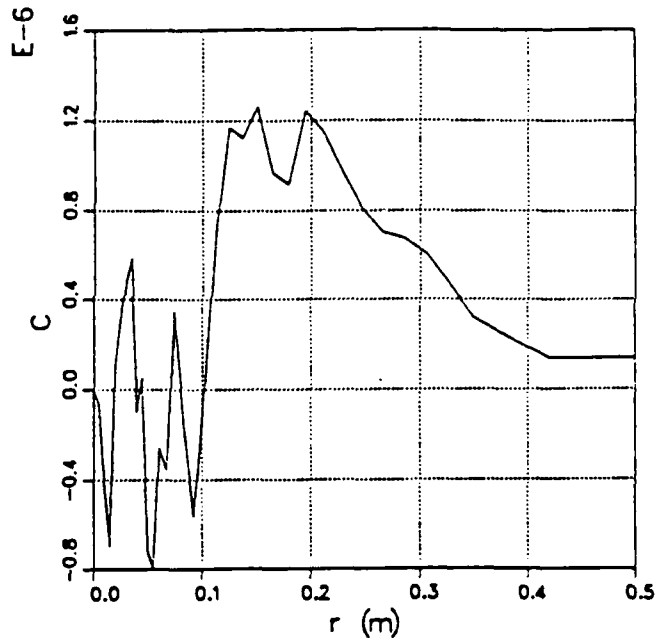


Figure 3.3. Radial integrals of current and charge in a simulated plasmoid; note that both integrals peak at roughly .15 meters radius and then decline to near zero. This shows core-halo division as expected. Note also that, inexplicably, net current is negative, while net charge is positive.

radiating excess energy and particles as it relaxes. By providing an excess of electrons, we provide an avenue for the escape of energy. The slight imbalance of negative charge also insures that electrons will not be emitted from the boundaries of the problem and come "crashing in" from large radii to the plasmoid, heating and disrupting it.

SECTION 4

THREE-DIMENSIONAL PLASMOID SIMULATIONS

4.1 SIMULATIONS USING THE CODE SOS

Plasmoid calculations were attempted in full three-dimensional space using the fully electromagnetic PIC code SOS⁴. The code SOS can operate on the Los Alamos Cray and can perform plasma simulations in fully three-dimensional space. SOS is similar to the code MAGIC, and the algorithms used to form plasmoids: the beam forming and programmed emission software, could be moved from MAGIC to SOS. The only major difference between the SOS and MAGIC simulations was a factor of four lower internal temperature in the plasmoids simulated by SOS together with lower net currents and charge densities compared to the MAGIC simulations. These measures allowed successful plasmoid creation using SOS.

Initial success was achieved in forming and propagating plasmoids of several meters, using models from MAGIC; however, the Los Alamos operating system was undergoing changes during this period and these changes, having to do with data allocation, began causing simulations to terminate prematurely without being able to recover. This behavior began abruptly and caused runs that had formerly run without difficulties to terminate in their late stages. These problems forced us to run only short simulations and consumed much time as we tried to remedy the problems encountered in long runs. As a result, only a few plasmoid simulations could be done successfully. Therefore, the successful simulations must be regarded as preliminary results, although the plasmoid behavior observed was very similar to that observed in the MAGIC simulations using rotational symmetry.

Despite the preliminary nature of the SOS results, it is of interest that SOS allowed cross sections of the plasmoid structure to be seen easily. These cross

sections confirmed the core-halo structure of the plasmoid, showing a hollow sheath surrounding a diffuse core. Evidence for an $m=4$ bunching in the halo was also seen.

A background magnetic field of 1 gauss was applied in the simulations; however, the simulations that were successfully completed did not run long enough to show electron dynamics through an electron cyclotron period. Unfortunately, longer runs would not complete due to abrupt changes in the Los Alamos system. The electron cyclotron period is 3.57×10^{-7} seconds, and the successful simulations lasted only 3×10^{-8} seconds. This means that effects due to the Earth's magnetic field, which we had desired to simulate and which would occur on time scales of an electron cyclotron period, will not appear.

4.2 RESULTS OF SIMULATIONS

The results of the plasmoid simulations can be summarized by the following output: x_2, x_3 (z, y) gridding for the plasmoid runs is shown in Figure 4.1. The plasmoid was launched in the x_1 (x) direction from the x_2, x_3 (z, y) plane. Only the top half of the gridding in the x_2, x_3 (z, y) plane is shown. The gridding for the x_1 (x) direction is uniform. The four-fold symmetry of the gridding may form an $m = 4$ perturbation that predisposes the halo to form this pattern late in the simulation. The rectangular gridding reflects the fact that the simulation was done in cartesian coordinates to avoid the singular behavior that occurs at $r = 0$. The formation and propagation of the plasmoid is seen from the side in Figures 4.2 and 4.3. Cross sections of the plasmoid showing its radial structure at origin and at the end of propagation distance are seen in Figures 4.4 and 4.5. It can be seen that a core and halo structure exists in these simulations and that a possible $m \approx 4$ filamentation of the halo has occurred after propagation of 2.5 meters, although this effect may be imposed by the four-fold symmetry of the gridding.

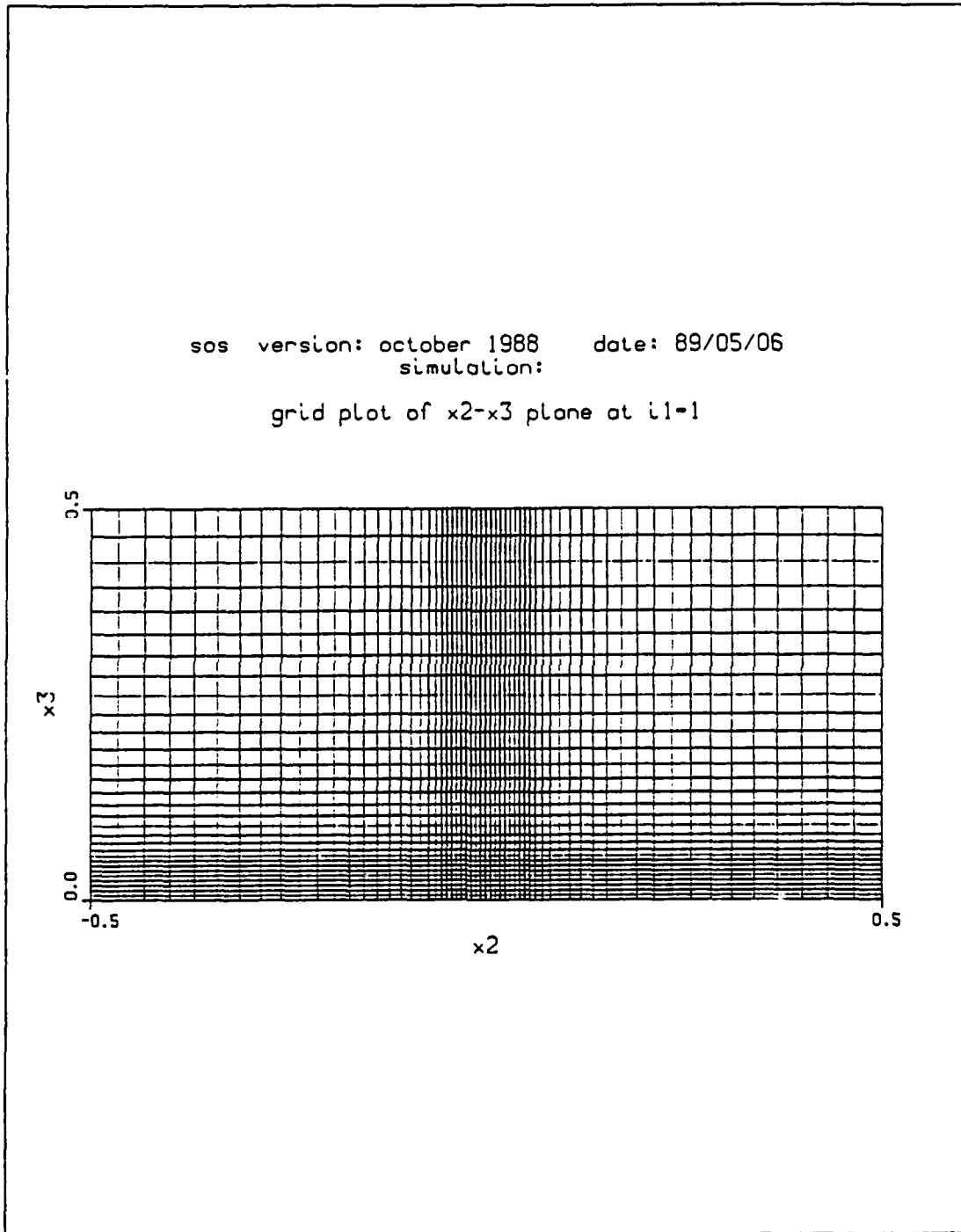


Figure 4.1. The x_2, x_3 (z, y) gridding of the plasmoid problem. Gridding in the x_1 (x) direction is uniform. Only the top half of the x_2, x_3 gridding is shown. 4-3

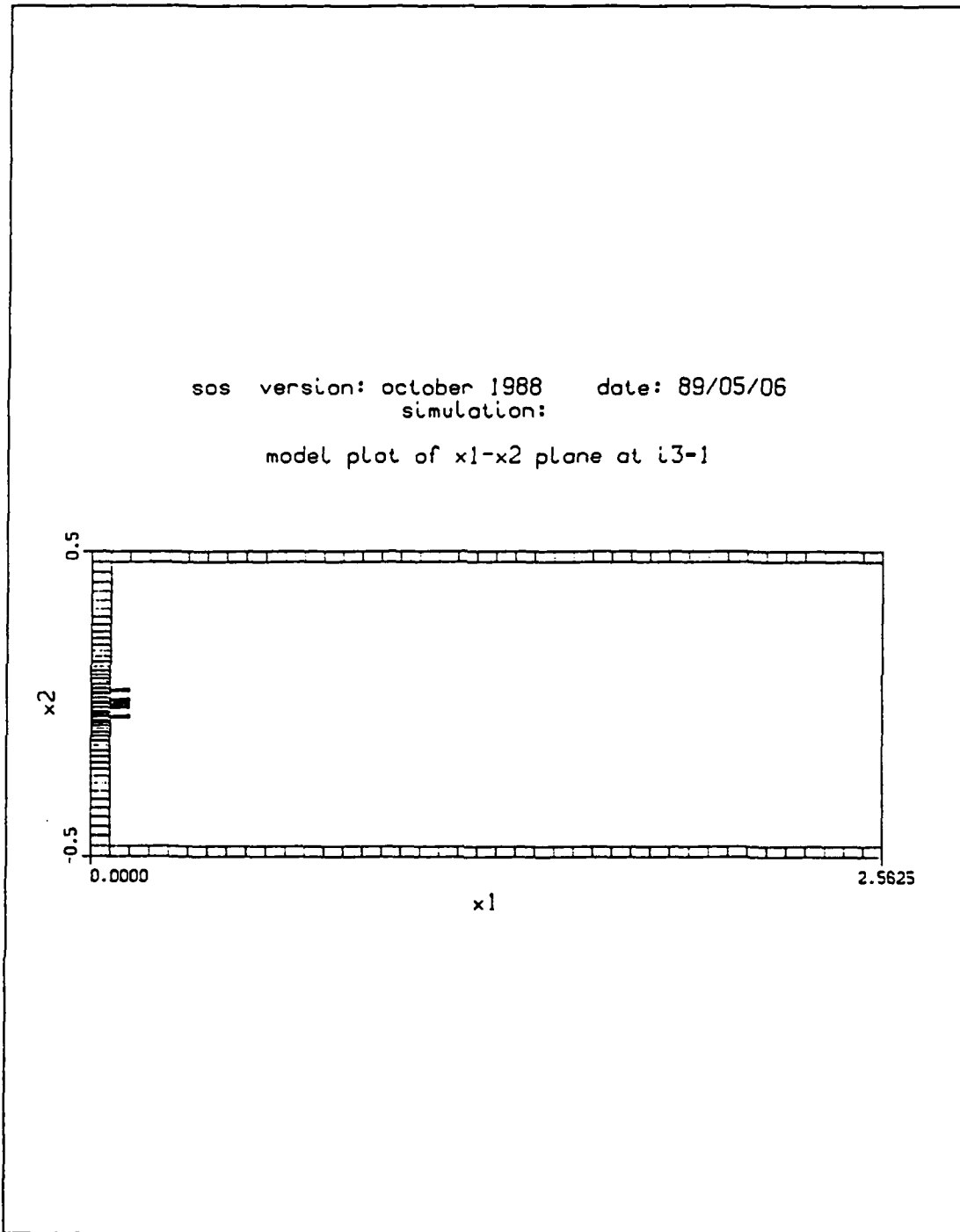


Figure 4.2. The initial beams for forming the plasmoid as they are emitted.

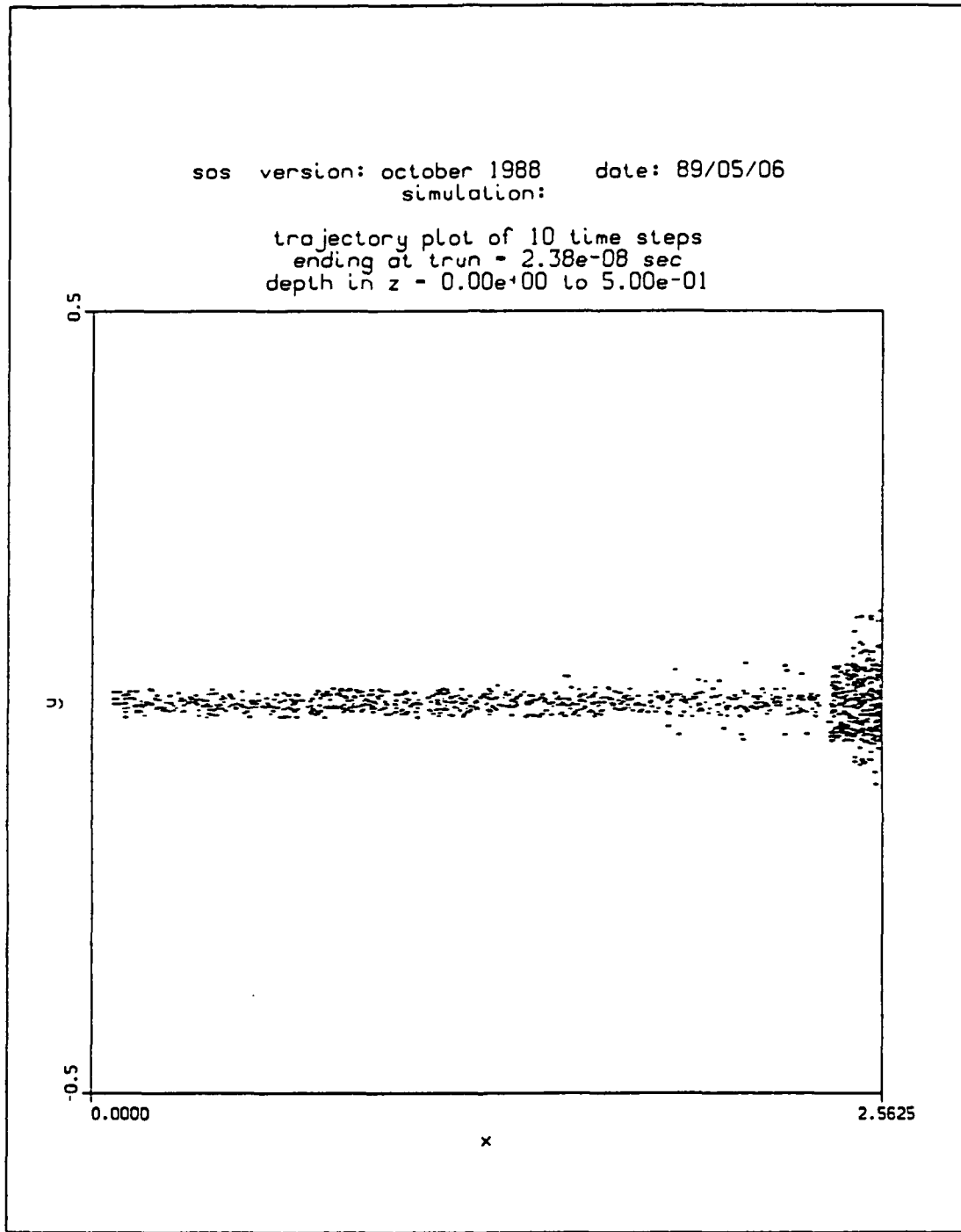


Figure 4.3. Final trajectory plots for a plasmoid. The plasmoid is seen impacting on the wall at 2.5 meters in. The trail of particles behind the plasmoid is a group of electrons and ions emitted after main beam shut down and are considered spurious since their total charge and current is negligible.

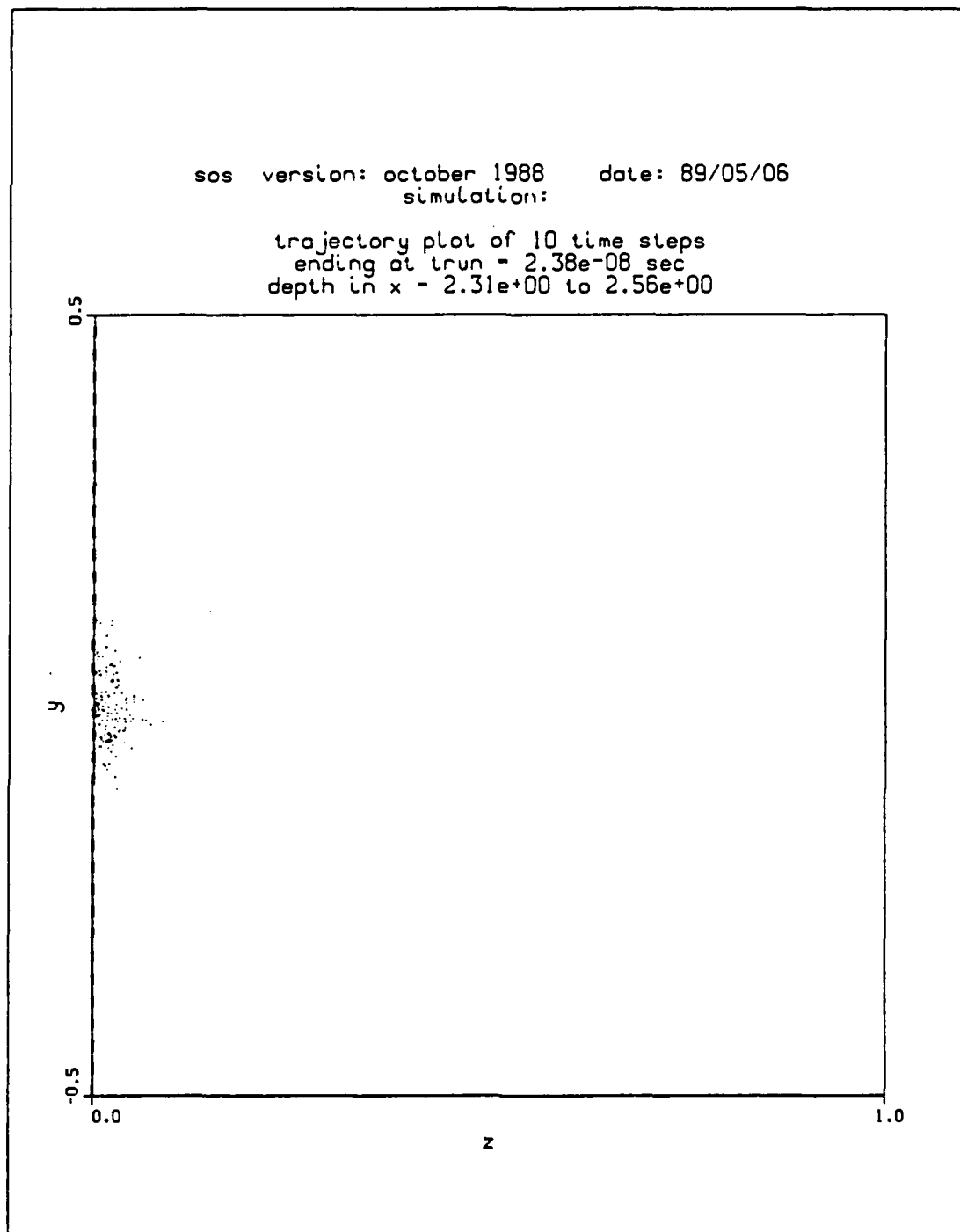


Figure 4.4. Cross section of the plasmoid at impact at 2.5 meters. The cross section shows clear core-halo structure with the suggestion of $m = 4$ filamentation in the halo.

SECTION 5

SUMMARY AND CONCLUSIONS

The effort to understand plasmoid formation and propagation has been largely successful. The Arrow model of the plasmoid, consisting of a pinched core and an expanding halo, appears to form and propagate stably when launched properly. However, one of the original goals, the demonstration of significant propagation of a plasmoid across a magnetic field, was not achieved. Despite this, progress was made in three areas:

1. An analytic model of core-halo dynamics was formed and was able to duplicate results of earlier simulations. This model gives the result that

$$a \sim (\ln R/a_0)^{3/2} \quad (5.1)$$

where a and a_0 are the core radius and initial core radius, respectively, and R is the halo radius. We also have

$$R \sim V_{th} t \quad (5.2)$$

where V_{th} is the core initial thermal velocity and t is time. These results suggest that plasmoids can propagate for long distances and still maintain a tightly pinched core, since the core radius will expand roughly as $a \sim (\ln t)^{3/2}$ late in time.

2. Formation of plasmoids requires initialization of current while avoiding the possibility of large charge separations. This was done by initially launching a plug of neutral plasma with electrons and ions at the same forward velocity and beam spread, followed by a core and halo set of beams consisting of electrons and ions at slightly ($\sim 5\%$) differing velocities and with a slight imbalance of charge. In the

core this charge imbalance favors the ions but electrons carry more current, and in the halo the opposite arrangement between electrons and ions occurs, except that the electrons are slightly more abundant than would give total charge balance to the plasmoid. The plasmoid thus sheds electrons initially. A final charge and current neutral plug of plasma is emitted to complete the plasmoid.

3. Propagation of plasmoids as a core-halo system for distances of meters has been demonstrated in two and half dimensions. Preliminary results of plasmoid propagation in three dimensions indicate that such propagation is possible for meters with the possibility of filamentation occurring in the halo.

In conclusion, our studies strongly suggest that the Arrow model of a plasmoid warrants further study and might also be a candidate for experimental study.

REFERENCE

1. J. E. Brandenburg and K. Wahlstrand, "Proceedings of SPIE (The International Society for Optical Engineering)," Vol. 873, p. 271, 1988.
2. T. R. Lockner, R. J. Lipinski, and R. B. Miller, "Plasmoid Propagation," Sandia Report SAND85-0917.
3. B. Goplen, L. Ludeking, J. McDonald, G. Warren, and R. Worl, "MAGIC User's Manual/Version - September 1988," Mission Research Corporation Report, MRC/WDC-R-184, September 1988.
4. Bruce Goplen, Kevin Heaney, James McDonald, Gary Warren, and Richard Worl, "SOS User's Manual - Version October 1988," Mission Research Report, MRC/WDC-R-158, 1988.